UDC 551.509.313:528.235

Conservative Finite-Difference Approximations of the Primitive Equations on Quasi-Uniform Spherical Grids

ROBERT SADOURNY—*Laboratoire de Météorologie Dynamique du C.N.R.S., Paris, France*

ABSTRACT—A class of conservative finite-difference approximations of the primitive equations is given for quasi-uniform spherical grids derived from regular polyhedrons. The earth is split into several contiguous regions. Within each region, a coordinate system derived from central projections is used, instead of the spherical coordinate system, to avoid the use of inconsistent boundary conditions at the poles. The presence of artificial internal boundaries has no effect on the conservation properties of the approximations. Examples of conservative schemes, up to the second order in the case of a cube, are given. A selective damping operator is needed to remove the two-grid interval waves generated by the existence of internal boundaries.

1. INTRODUCTION

The numerical integration of the equations of atmospheric motion requires the definition of a system of scalar equations with an appropriate coordinate system. However, when we try a complete description of the flow over the whole sphere, a single coordinate system is clearly insufficient inasmuch as the sphere is not homeomorphic to the plane. It is necessary to split the complete spherical domain into several open regions. For instance, Phillips (1959) suggested the use of two polar caps together with an equatorial belt. In the most commonly used method, the two caps are restricted to the immediate vicinity of the poles, which allows the use of spherical coordinates over almost the whole domain. However, artificial boundary conditions are necessary in both cases. In the method described by Phillips, there is an overlapping of the grids in the middle latitudes, and one needs to interpolate values from one grid to its neighbor in the course of the calculation. This need makes the design of a globally conservative scheme impossible in practice. When the equatorial belt extends to the vicinity of the poles, interpolations are no longer necessary. However, the two poles are singular points in the spherical coordinate system, and the design of a boundary condition in their close vicinity is a delicate matter.

When spherical coordinates are used except in the immediate vicinity of the poles, the most natural choice is a uniform grid in the longitude-latitude plane. However, such a grid is quite inefficient from the computational standpoint because of its exceedingly high resolution at higher latitudes. The use of other grids with a more uniform spacing on the sphere has been suggested by several authors. Such were the Kurihara (1965) and Kurihara and Holloway (1967) grids in which the number of gridpoints along a parallel circle decreases from Equator to pole. Later, the use of a quasi-uniform spherical grid derived from the icosahedron was suggested by Sadourny et al. (1968) and by Williamson (1968, 1970). In these grids, the pole is surrounded by a fixed number of gridpoints (four in the case of Kurihara's grids, five for the icosahedral grid). In other words, the increment in longitude, $\Delta\lambda$, between these gridpoints stays at a fixed value ($\Delta\lambda=\pi/2$ or $\Delta\lambda=2\pi/5$) instead of decreasing with the grid size.

2. THE BOUNDARY CONDITION AT THE POLE IN SPHERICAL COORDINATES

We shall investigate the boundary condition at the pole when spherical coordinates are used. The zonal component of the equation of motion in the case of a two-dimensional barotropic flow is then

$$\frac{\partial u}{\partial t}(\lambda, \varphi, t_0)+A(\lambda, \varphi, t_0)=0$$

with

$$A(\lambda, \varphi, t_0)=\frac{1}{a}\left[\frac{u}{\cos\varphi}\left(\frac{\partial u}{\partial\lambda}-v\sin\varphi\right)+v\frac{\partial u}{\partial\varphi}+\frac{\lambda}{\cos\varphi}\frac{\partial\phi}{\partial\lambda}\right]-vf$$

where t_0 is the time, λ the longitude, φ the latitude, u and v the zonal and meridional components of the wind velocity vector, a the radius of the earth, f the Coriolis parameter, and ϕ the geopotential. When λ is held constant ($\lambda=\lambda_0$) and $\varphi\to\pi/2$, the quantity $A(\lambda,\varphi,t_0)$ has a finite limit:

$$B(\lambda_0, t_0)=\lim_{\varphi\to\frac{\pi}{2}} A(\lambda_0, \varphi, t_0)\cdot$$

Then the equation

$$\frac{\partial u}{\partial t}\left(\lambda_0, \frac{\pi}{2}, t_0\right)+B(\lambda_0, t_0)=0$$

defines one component of the time derivative of the wind velocity vector at the North Pole.

Let us define a parameter d as the grid distance in the (φ,λ) plane when we use a regular grid, G, on this plane, or as the smallest grid distance if the grid G is not regular. A finite-difference approximation, $\delta u/\delta\lambda(\lambda,\varphi,t_0,d)$, of $\partial u/\partial\lambda(\lambda,\varphi,t_0)$ defined on G is consistent when the condition

$$\lim_{d\to 0}\frac{\delta u}{\delta\lambda}\left(\lambda,\varphi,t_0,d\right)=\frac{\partial u}{\partial\lambda}\left(\lambda,\varphi,t_0\right)$$

is satisfied at every gridpoint. On the other side, a consistent approximation $A^*(\lambda,\varphi,t_0,d)$ of $A(\lambda,\varphi,t_0)$ is such that

$$\lim_{d\to 0}A^*(\lambda,\varphi,t_0,d)=A(\lambda,\varphi,t_0)$$

at every gridpoint but the polar gridpoints, and

$$\lim_{\substack{d\to 0\\ \varphi\to\frac{\pi}{2}}}A^*(\lambda,\varphi,t_0,d)=B(\lambda,t_0).$$

We can see readily that, if we define the approximation for the u component of the equation of motion as

$$A^*(\lambda,\varphi,t_0,d)=\frac{1}{a}\left[\frac{u}{\cos\varphi}\left(\frac{\delta u}{\delta\lambda}-v\sin\varphi\right)+v\frac{\partial u}{\partial\varphi}+\frac{1}{\cos\varphi}\frac{\delta\phi}{\delta\lambda}\right]-vf,$$

the consistency of $\delta u/\delta\lambda$ alone is not sufficient to ensure consistency for A^*. An obvious sufficient condition is the following:

$$\lim_{\substack{d\to 0\\ \varphi\to\frac{\pi}{2}}}\frac{1}{\frac{\pi}{2}-\varphi}\left(\frac{\delta u}{\delta\lambda}-\frac{\partial u}{\partial\lambda}\right)=0.$$

This condition is not verified when the grid is quasi-uniform on the sphere since the necessary condition

$$\lim_{\substack{d\to 0\\ \varphi\to\frac{\pi}{2}}}\left(\frac{\delta u}{\delta\lambda}-\frac{\partial u}{\partial\lambda}\right)=0$$

is not even met. For a uniform grid in the (φ,λ)-plane, at least a second-order scheme is required in the vicinity of the pole.

The choice of spherical coodinates is not a suitable choice when one decides to use a quasi-uniform grid for reasons of computational efficiency. The alternative we propose is the choice of central projections, chosen in such a way that they map the whole sphere onto a regular polyhedron. Although the mapping is not conformal, the scalar equations are rather simple. The boundary conditions are seen to vanish in the finite-difference formulation, and the simplest schemes are mass- and energy-conserving. Consistency as well as computational efficiency are easy to obtain in the absence of singularities.

3. THE EQUATIONS IN A POLYHEDRAL REPRESENTATION OF THE EARTH

Let us consider the basic equations for a two-dimensional free surface flow on the sphere in the following form:

$$\frac{\partial\mathbf{V}}{\partial t}+\mathbf{k}\times\mathbf{V}(f+\text{curl }\mathbf{V})+\text{grad}\left(\phi+\frac{1}{2}\mathbf{V}^2\right)=0$$

and

$$\frac{\partial\phi}{\partial t}+\text{div }(\phi\mathbf{V})=0 \tag{1}$$

where $\mathbf{V}$ is the wind velocity vector and $\mathbf{k}$ the unit vector normal to the sphere. In the first equation, the curl of a two-dimensional vector field has been identified with a scalar. Let P be a regular polyhedron circumscribed to the sphere S, P_n $(n=1,\ p)$ be one of its faces, F_n the central projection of P_n onto the sphere, and S_n the image $S_n=F_n(P_n)$. The family $(P_n,\ F_n)_{n=1,\,p}$ may be called a (polyhedral) representation of S. If we denote by P_{nm} the intersection between P_n and P_m, which may be void if P_n and P_m are not contiguous, then the boundary of P_n is exactly the reunion of all P_{nm} for all m. Furthermore, the mappings F_n and F_m do coincide on P_{nm} and the common boundary of S_n and S_m is

$$S_{nm}=F_n(P_{nm})=F_m(P_{nm}). \tag{2}$$

This particular representation of S will allow us to write scalar analogs of eq (1) as a set of scalar partial differential equations, each valid in a domain P_n.

Since F_n is not a conformal mapping, we shall have to introduce the general formulation of elementary differential geometry.

Let m be any point in P_n, x^i $(i=1,\ 2)$ its coordinates in a Cartesian system, and $\mathbf{M}=F_n(m)$ its image in S_n. Then any vector field $\mathbf{V}(\mathbf{M})$ in S_n is entirely defined by its covariant or contravariant components u_i and u^i:

$$u_i=\mathbf{V}\cdot\frac{\partial\mathbf{M}}{\partial x^i}$$

and

$$\mathbf{V}=u^i\frac{\partial\mathbf{M}}{\partial x^i}.$$

(The usual summation convention will be used throughout this paper.) The local geometry is described by the (g_{ij}) tensor:

$$g_{ij}=\frac{\partial\mathbf{M}}{\partial x^i}\cdot\frac{\partial\mathbf{M}}{\partial x^j}$$

and

$$g=\frac{\partial\mathbf{M}}{\partial x^1}\times\frac{\partial\mathbf{M}}{\partial x^2}=[\det(g_{ij})]^{1/2}.$$

Here, we identify the cross-product of two 2-dimensional vectors with a scalar and specify that the determinant, (det), of (g_{ij}) has a positive value. Then we are able to

express the scalar and cross-products of two vectors **A** and **B** as:

$$\mathbf{A}\cdot\mathbf{B}=a_ib^i$$

and

$$\mathbf{A}\times\mathbf{B}=\left|\begin{matrix}a^1a^2\\b^1b^2\end{matrix}\right|\frac{\partial\mathbf{M}}{\partial x^1}\times\frac{\partial\mathbf{M}}{\partial x^2}=g\left|\begin{matrix}a^1a^2\\b^1b^2\end{matrix}\right|$$

where a_i, b_i and a^i, b^i are the covariant and contravariant coordinates of **A** and **B**.

When the origin in P_n is the center of the face, we get

$$g_{ij}=\frac{r^2}{a^4}\begin{pmatrix}(x^1)^2+a^2 & -x^1x^2\\ -x^1x^2 & (x^2)^2+a^2\end{pmatrix}$$

where a is a radius of the earth and $r^2=a^2+(x^1)^2+(x^2)^2$.

Let $d\mathbf{S}$ be a curve element in S_n, and ds^i its contravariant components. The circulation of **V** along the curve element is defined as the invariant differential form

$$\mathbf{V}\cdot d\mathbf{S}=u_ids^i.$$

The flux through $d\mathbf{S}$ is also an invariant differential form:

$$\mathbf{V}\times d\mathbf{S}=g\left|\begin{matrix}u^1u^2\\ds^1ds^2\end{matrix}\right|$$

which does not depend on the mapping. These relations, together with Stokes' theorem applied to an infinitesimal square parallel to the coordinate lines, lead to the expressions

$$g\ \text{curl}\ \mathbf{V}=\epsilon^{ij}\frac{\partial u_j}{\partial x^i}$$

and

$$g\ \text{div}\ \mathbf{V}=\frac{\partial}{\partial x^i}(gu^i)$$

where

$$(\epsilon_{ij})=(\epsilon^{ij})=\begin{pmatrix}\epsilon^{11}\epsilon^{12}\\ \epsilon^{21}\epsilon^{22}\end{pmatrix}=\begin{pmatrix}0 & 1\\ -1 & 0\end{pmatrix}.$$

We are now able to write scalar analogs of eq (1) in P_n; that is,

$$\frac{\partial u_i}{\partial t}+\epsilon_{ij}gu^j\left(f+\frac{1}{g}\epsilon^{kl}\frac{\partial u_l}{\partial x^k}\right)+\frac{\partial}{\partial x^i}\left(\phi+\frac{1}{2}u_ku^k\right)=0$$

and (3)

$$g\frac{\partial\phi}{\partial t}+\frac{\partial}{\partial x^i}(g\phi u^i)=0.$$

(The first equation is obtained after scalar multiplication of the equation of motion by $\partial\mathbf{M}/\partial x_i$.)

It should be noticed that the use of a conformal mapping would not lead to a simpler expression. To close the system, however, we need the expression of the contravariant components

$$u^i=g^{ij}u_j$$

where (g^{ij}) is the inverse of the matrix (g_{ij}). In a conformal mapping, these matrices would be diagonal.

We shall need now a description of the conservation mechanisms for mass and energy in the representation (P_n, F_n). Let us write the time derivative of the total energy per unit area in P_n:

$$g\frac{\partial E}{\partial t}=g\frac{\partial}{\partial t}\left(\frac{1}{2}\phi^2+\frac{1}{2}\phi u_ku^k\right)=\left(\phi+\frac{1}{2}u_ku^k\right)g\frac{\partial\phi}{\partial t}+(g\phi u^k)\frac{\partial u_k}{\partial t}.$$

When we use eq (3) for $\partial\phi/\partial t$ and $\partial u_k/\partial t$, the following identity results:

$$g\frac{\partial E}{\partial t}+\frac{\partial}{\partial x^i}\left[\left(\phi+\frac{1}{2}u_ku^k\right)g\phi u^i\right]=0.$$

Setting $a=\phi+\frac{1}{2}u_ku^k$ and $b=g\phi u^i$, we see that the only property used in this derivation is the formal differentiation property

$$a\frac{\partial}{\partial x^i}b+b\frac{\partial}{\partial x^i}a=\frac{\partial}{\partial x^i}(ab). \tag{4}$$

If we denote by E_n and ϕ_n the space integrals of E and ϕ over the whole domain, P_n (we may notice that ϕ_n is proportional to the space integral of the mass over P_n), Stokes' theorem leads to the expressions

$$\frac{\partial E_n}{\partial t}+\sum_m\oint_{P_{nm}}\left(\phi+\frac{1}{2}u_ku^k\right)g\phi\left|\begin{matrix}u^1u^2\\ds^1ds^2\end{matrix}\right|=0$$

and (5)

$$\frac{\partial\phi_n}{\partial t}+\sum_m\oint_{P_{nm}}g\phi\left|\begin{matrix}u^1u^2\\ds^1ds^2\end{matrix}\right|=0.$$

As we sum over n to get the integrated energy and geopotential over the whole sphere, eq (2) together with the invariance of the flux differential form with respect to the mapping will cause all line integrals to cancel one another exactly.

4. CONSERVATIVE FINITE-DIFFERENCE APPROXIMATIONS

Let the operators curl*, grad*, and div* be finite-difference approximations of the spherical differential operators curl, grad, and div. Then the expressions

$$\frac{\partial\mathbf{V}}{\partial t}+\mathbf{k}\times\mathbf{V}(f+\text{curl*}\ \mathbf{V})+\text{grad*}\left(\phi+\frac{1}{2}\mathbf{V}^2\right)=0$$

and (6)

$$\frac{\partial\phi}{\partial t}+\text{div*}\ (\phi\mathbf{V})=0$$

are a finite-difference approximation of eq (1).

To get such an expression we introduce a regular grid Π_n within a face P_n. We are then able to substitute usual finite-difference operators, $\delta/\delta x^i$, for the differential operators, $\partial/\partial x^i$, in eq (3). The linear operator, $\delta/\delta x^i$, can be described by a $N\times N$ matrix, where N is the number of gridpoints in Π_n. Then

$$\frac{\partial u^i}{\partial t}+\epsilon_{ij}u_j\left(gf+\epsilon^{kl}\frac{\delta u_l}{\delta x^k}\right)+\frac{\delta}{\delta x^i}\left(\phi+\frac{1}{2}u_ku^k\right)=0$$

and (7)

$$g\frac{\partial\phi}{\partial t}+\frac{\delta}{\delta x^i}(g\phi u^i)=0$$

are possible expressions for eq (6) at any gridpoint which belongs to Π_n.

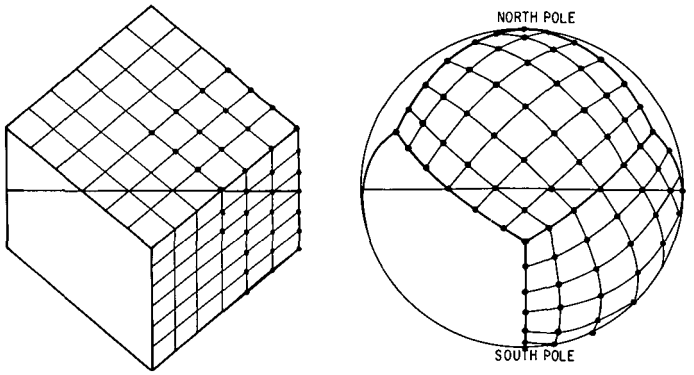

FIGURE 1.—A cubic representation of the earth. A cubic grid is shown together with the corresponding spherical grid which fits into the cubic splitting of the sphere, in the exact disposition that was used in the actual computations.

In section 3, we had contiguous faces that proved to be useful in the description of the conservation mechanisms. We shall ask similar properties from the grids Π_n. Mainly, they should be contiguous in the following sense: if we denote by Π_{nm} the intersection between Π_n and Π_m, which may be void if Π_n and Π_m are not contiguous, we shall ask that the boundary (in the grid sense) of Π_n be exactly the reunion of all Π_{nm} for all m. This means that the gridpoints which belong to an edge P_{nm} are common to both grids Π_n and Π_m (fig. 1). Then F_n and F_m do coincide on the grid boundary Π_{nm}, and the intersection between the spherical grids $\Sigma_n=F_n(\Pi_n)$ and $\Sigma_m=F_m(\Pi_m)$ is

$$\Sigma_{nm}=F_n(\Pi_{nm})=F_m(\Pi_{nm}). \tag{8}$$

For the gridpoints which belong to Σ_{nm}, we get two different finite-difference forms [eq (7)] (one involving F_n and gridpoints in Π_n, another involving F_m and the gridpoints in Π_m) or even more if the gridpoint is a vertex. In these cases, we define the final form [eq (6)] from an equally weighted average of these possible approximations.

We shall be interested only in conservative approximations; by a conservative approximation, we mean that the approximation is such that some discrete forms of the total energy and total geopotential are exactly conserved in the time integration. Discrete approximation of E_n and ϕ_n may be given by the expressions

$$E_n^*=\sum_{\Pi_n}\lambda g\left(\frac{1}{2}\phi^2+\frac{1}{2}\phi u_k u^k\right)$$

and

$$\phi_n^*=\sum_{\Pi_n}\lambda g\phi$$

where the coefficients λ are weight coefficients that define the discrete form of the space integral. Their sum over Π_n is the area of P_n, but they need not be the same at all points.

In the continuous case, the mechanism of energy conservation inside P_n has been described by eq (4). In fact, we only need the discrete analog of the spatial integral of eq (4):

$$\sum_{\Pi_n}\left[a\left(\lambda\frac{\delta}{\delta x^i}\right)b+b\left(\lambda\frac{\delta}{\delta x^i}\right)a\right]=\sum_m\sum_{\Pi_{mn}}(aB_ib). \tag{9}$$

The second member is the most general bilinear form depending only on boundary values. The linear operator B_i may be described by a matrix β_i:

$$\beta_i=(\beta_i^{rs})_{r=1,N;s=1,N}$$

with $\beta_i^{rs}\neq 0$ only when r and s refer to a boundary point. The general solution of eq (9) when the second member is null is any antisymmetric bilinear form $\sum_{\Pi_n}(aA_ib)$ where A_i is a linear operator described by any antisymmetric matrix α_i where

$$\alpha_i=(\alpha_i^{rs})_{r=1,N;s=1,N}$$

with $\alpha_i^{rs}=-\alpha_i^{sr}$. Hence, the general solution of eq (9) is

$$\left(\lambda\frac{\delta}{\delta x^i}\right)=A_i+B_i. \tag{10}$$

The splitting property [eq (10)] ensures that the mechanism of energy conservation holds within Π_n. In fact, mass conservation also follows from eq (10). To show this, we need only substitute $a=1$ for $a=\phi+\frac{1}{2}u_ku^k$ and use the same argument, with the further condition that $\delta(1)/\delta x^i=0$, which is verified, in any case, for a consistent approximation.

The splitting condition [eq (10)] is indeed Stokes' theorem in finite-difference form. We may then express the time derivative of E_n^* (respectively ϕ_n^*). In both cases, it reduces to a discrete approximation of the outgoing flux of energy (respectively geopotential) on the boundary of Π_n that depends on boundary values only. That is,

$$\frac{\partial E_n^*}{\partial t}+\sum_m\sum_{\Pi_{mn}}\left(\phi+\frac{1}{2}u_ku^k\right)B_i(g\phi u^i)=0$$

and

$$\frac{\partial\phi_n^*}{\partial t}+\sum_m\sum_{\Pi_{mn}}B_i(g\phi u^i)=0. \tag{11}$$

These equations are the exact analogs of eq (5). Contrary to what happened in section 1, the fact that the grids are exactly contiguous, expressed by eq (8), together with the invariance properties of the flux form with respect to the mapping, are not sufficient to ensure the exact cancellation of the boundary terms as we sum over n. We need the further condition that the *discrete forms* of the line integral described by the operator B_i be the same on both sides of the boundary.

To meet this condition, it is not sufficient to require that the scheme should be the same in all faces. In fact, the faces meet one another in many ways. In the case of a cube, for instance, a boundary, P_{nm}, may be parallel to the x^1 coordinate lines in the square P_n and parallel to the x^2 coordinate lines in P_m. In the case of an icosahedron or any polyhedron with triangular faces, the junction occurs in several ways since the boundaries are parallel to three directions y^1, y^2, and y^3. In the case of a cube, the invariance condition on B_i will be verified if the scheme is

formally the same in both directions: a single one-dimensional operator $\delta/\delta x$ should be used for the definition of $\delta/\delta x^1$ and $\delta/\delta x^2$. Such a scheme may be called isotropic with respect to the grid. We get a similar condition in the case of a triangular grid: $\delta/\delta y^j$ where $j=1, 3$ are defined by a single one-dimensional operator $\delta/\delta y$. Then an isotropic scheme has the following form:

$$\frac{\delta}{\delta x^i}=\frac{2}{3}\cos(\theta_i^j)\frac{\delta}{\delta y^j}\ (i=1,2;\ j=1,3).$$

The general form of a conservative scheme is then an isotropic scheme deduced from a one-dimensional approxition satisfying the splitting condition [eq (10)]. Here, we may recall that the scheme on an internal boundary Π_{nm} is an averaged form of the schemes in Π_n and Π_m. In the average, the boundary terms (depending on the operators B_t) vanish as they do in the space integrals, and for the same reasons. The final approximation is thus completely determined by a one-dimentional antisymmetric operator, A; the presence of internal boundaries is not explicit in the calculations.

5. FIRST- AND SECOND-ORDER APPROXIMATIONS

The antisymmetric operator A is described by a matrix $\alpha=(\alpha^{rs})$, with $\alpha^{rs}=-\alpha^{sr}$. We call A a uniform scheme when

$$\alpha^{r,\,r+q}=\alpha^{s,\,s+q}.$$

These two relations yield

$$\alpha^{r,\,r+q}=-\alpha^{r-q,\,r}$$

which means that a uniform antisymmetric scheme is what we usually call a centered scheme. Hence, any centered scheme is a conservative scheme.

The simplest conservative approximation is then deduced from the usual 3-point centered scheme. The difference operator acting on any row of gridpoints within a face is described by a matrix

$$\alpha=\left[\begin{array}{cccc:c} 0 & 1 & 0 & 0 & \\ -1 & 0 & 1 & 0 & \\ 0 & -1 & 0 & 1 & \\ 0 & 0 & -1 & 0 & \\ \hdashline & & & & \end{array}\right].$$

The boundary operator B in this case would be described by the matrix

$$\beta=\left[\begin{array}{ccc:c} -1 & 0 & 0 & 0 \\ 0 & 0 & 0 & 0 \\ 0 & 0 & 0 & 0 \\ \hdashline 0 & 0 & 0 & 1 \end{array}\right]$$

and the weights, λ, should have the values

$$\lambda=(d,\ 2d,\ 2d,\ \ldots,\ 2d,\ d).$$

Then the operator $\delta/\delta x$ given by

$$\left(\lambda\frac{\delta}{\delta x}\right)=\alpha+\beta$$

is a second-order operator everywhere except at the extremities of the row. The finite-difference form [eq (7)] is then a first-order approximation on the boundaries, Π_{nm}, and a second-order approximation everywhere else. The averaging process that defines the final form of the approximation on the boundaries, although it leads to a formally centered scheme with vanishing of all boundary terms, does not restore second-order accuracy; the first-order error on each side is dependent on the mapping and does not cancel in the average.[1] However, if M is the total number of gridpoints and M' the number of boundary points, M' is small compared to M. In fact,

$$\frac{M'}{M}=O(d)$$

where d is grid size of Π_n. The global average of the magnitude of the truncation error may be estimated as

$$\sigma=[1-O(d)]O(d^2)+O(d)O(d)=O(d^2).$$

We shall, nevertheless, refer to this approximation as "a first-order" approximation, to emphasize its behavior on internal boundaries, and call it scheme I. We can expect the relatively large trunction error on the boundaries to act as an isolated perturbation of the flow and to generate a two-grid interval computational noise.

Since the averaging process cannot be expected to increase the accuracy on the boundaries, a true second-order scheme is a scheme where eq (7) is already a second-order approximation at all points of Π_n including those on Π_{nm}. In other words, the one-dimensional approximation δ/δ_x should be of second-order accuracy at the extremities of the row. For instance, the approximation defined by

$$\alpha=\left[\begin{array}{ccccc:c} 0 & 4 & -1 & 0 & 0 & \\ -4 & 0 & 4 & 0 & 0 & \\ 1 & -4 & 0 & 4 & -1 & \\ 0 & 0 & -4 & 0 & 4 & \\ 0 & 0 & 1 & -4 & 0 & \\ \hdashline & & & & & \end{array}\right],$$

$$\beta=\left[\begin{array}{ccc:c} -3 & 0 & 0 & 0 \\ 0 & 0 & 0 & 0 \\ 0 & 0 & 0 & 0 \\ \hdashline 0 & 0 & 0 & 3 \end{array}\right],$$

[1] Higher order centered schemes would still lead to a first-order scheme on the boundaries.

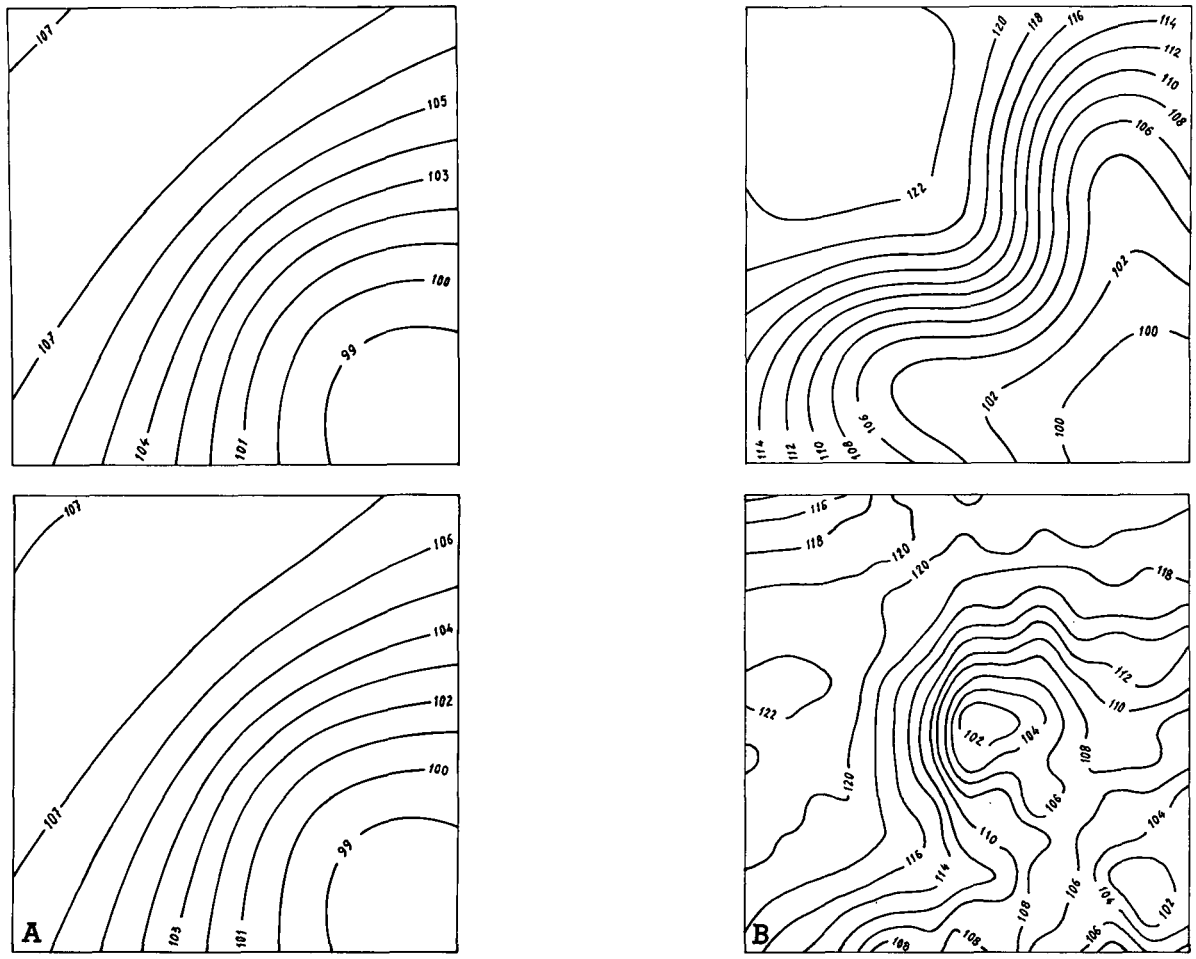

FIGURE 2.—Results from a numerical integration using the coarse grid and scheme II, showing the evolution of the geopotential field from day 0 (top) to day 5 (bottom) in the case of (A) solid rotation and (B) Phillips' wave. One face only is shown. The central projection is used for the map. The South Pole is located at the lower right corner. Units are $10^3 \cdot m^2 \cdot s^{-2}$.

and

$$\lambda = (2d,\ 8d,\ 4d,\ 8d,\ \ldots,\ 2d)$$

leads to a second-order conservative scheme. However, this operator requires an odd number of gridpoints on the row. It can be used on a $(2p+1)\times(2p+1)$ square grid, in the case of a cube, but cannot be used for polyhedrons with triangular faces since the number of gridpoints on a row is alternatively even and odd. The main defect of the scheme is the alternance in the finite-difference formulation for even and odd points and the alternance in the weights of the gridpoints. Hence, we can expect again a two-grid interval computational noise. This scheme on the cube will be called scheme II.

The numerical tests of the method were done on a cube to compare the second-order approximation to the first-order approximation. However, the cube is not necessarily the best choice among all polyhedrons. It is obvious that the dodecahedron has to be discarded since its faces are pentagons that are unfit for the design of a grid. The regular polyhedrons with triangular faces are the tetrahedron, the octahedron, and the icosahedron. The icosahedron is the most efficient from the computational standpoint. If we suppose we need to integrate the equations from $t=0$ to $t=T$ with a given maximum grid distance Δ on the sphere, using the simplest possible scheme (scheme I), the efficiency of a polyhedron can be measured by the actual time, $\theta(T, \Delta)$, needed for the integration. We can compute the following estimates: setting $\theta(T, \Delta)=\theta_0$ for the icosahedral grid, we get $\theta(T, \Delta)=1.7\theta_0$ for the octahedral or the cubic grid, and $\theta(T,\Delta)=8\theta_0$ for the tetrahedral grid. The rather large variation in grid size from the center of a face to a vertex is responsible for the low efficiency of the tetrahedron.

In the case of the first-order scheme, the first-order truncation error on the internal boundaries will be predominant. This truncation effect will depend on the parameter $\rho=M'/M$. Again, if we compare the various types of grids for a given maximum grid distance on the sphere, setting $\rho=\rho_0$ for the icosahedral grid, we get $\rho=0.55\rho_0$ for the octahedral grid, $\rho=0.6\rho_0$ for the cubic grid, and $\rho=0.67\rho_0$ for the tetrahedral grid. However, the truncation effect is too complex to be described by a single parameter. It is likely that the accuracy of the computations is not significantly affected by the choice of the polyhedron.

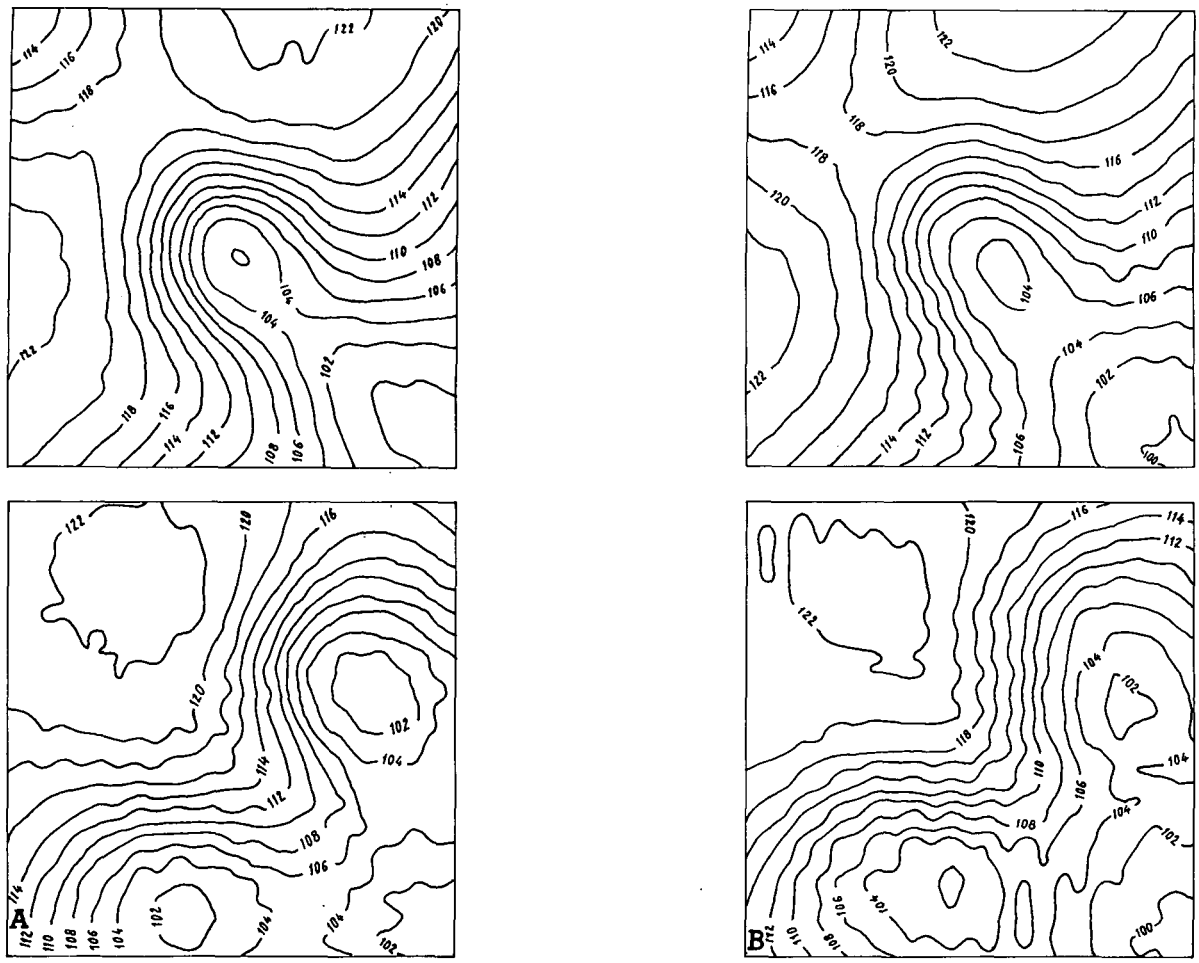

FIGURE 3.—Results on day 4 (top) and day 8 (bottom) from a numerical integration using the finer grid in the case of Phillips' wave using (A) scheme I and (B) scheme II. The mapping has the same disposition as in figure 2. Units are $10^3 \cdot m^2 \cdot s^{-2}$.

6. NUMERICAL TESTS OF THE METHOD ON A CUBE

The cube was mapped into the sphere in such a way that all six faces played the same role with respect to the axis of rotation. In this case, the two poles are the images of two opposite vertices (fig. 1). Two grids were designed on the cube: a coarse grid (866 points) corresponding to a maximum grid distance of roughly 1000 km at the center of each face and a finer grid (3,458 points) which corresponds to half that distance. The first tests were done using scheme II. We considered first the so-called "solid rotation" case with the following initial fields:

$$u = u_0 \sin \varphi,$$

$$v = 0,$$

and

$$\phi = \phi_0 + (a u_0 \Omega + \tfrac{1}{2} u_0^2) \cos^2 \varphi$$

where u and v are again the zonal and meridional components of the wind velocity vector, φ is the latitude, and Ω the angular velocity of the earth. We took $u_0 = 20$ m/s, $\phi_0 = 98{,}100$ $m^2 \cdot s^{-2}$. There was no significant growth of the noise after the second day although it reached such amplitude as 0.6 m/s for the wind field. The small-scale oscillations due to the scheme appeared as transient, without evidence of a large-scale disturbance (fig. 2A) if we expect a slight gravity oscillation effect from Equator to pole. The time derivation was approximated by the usual centered, or "leapfrog" scheme, with a 12-min time step.

A second series of experiments was then performed, using initial data close to those used by Phillips (1959). A nondivergent flow pattern was selected as an initial condition, derived from a stream function ψ:

$$\psi = -a^2 \omega \sin \varphi + a^2 \omega \cos^4 \varphi \sin \varphi \cos 4\lambda$$

where λ is the longitude and ω is equal to $7.48 \times 10^{-6} s^{-1}$. The exact balanced geopotential corresponding to this stream function is to be found in Phillips (1959). The solution that corresponds to this initial condition in the nondivergent case is a Haurwitz wave moving slowly from west to east with an angular velocity $\nu = 2\pi/29.3$, which leads to a time period close to 7.35 days. The same time extrapolation was used, but the time step had to be reduced to 8 min in the coarse grid case, due to the very large amplitude of the wind velocity. The use of the coarse

grid in this case led to a rather large amplitude of the two-grid interval noise (fig. 2B). The experiment was then repeated on the fine grid: two runs of 10 days each were performed to compare scheme I to scheme II (fig. 3). The noise is seen to be slightly less in the first case (fig. 3A). The phase speed is slightly slower with scheme II (fig. 3B), with an 8-day period instead of an 8.4-day period when scheme I is used. Both speeds are less than the predicted speed in the nondivergent case, which had to be expected. We know that the presence of a nonzero divergence contributes to slow down the rate of progression of large-scale waves.

Although scheme II is a uniformly second-order approximation, we can see that it is not an improvement on scheme I. In fact, the truncation error of scheme I, which is higher along the boundaries, is much less inside the faces, and its overall effect has the same magnitude. The two-grid interval noise seems to be inherent to the use of a conservative scheme in the presence of internal computational boundaries. (It goes without saying that we may increase the accuracy to the extent desired, provided we drop the conservation conditions.) It is interesting enough to compare these results to similar computations in the nondivergent case (Sadourny et al. 1968, Williamson 1968). Although it was not explicit in the formulation of the scheme, we had the same kind of truncation error in that case; the approximations used for the barotropic vorticity equation were of second-order accuracy inside the faces of the icosahedron; but they were of first-order accuracy only on the edges. The fact that the approximations did not actually generate a two-grid interval noise is easily explained by the exact conservation of enstrophy which, coupled to the exact conservation of energy, does not allow any artificial energy cascade whatsoever toward higher wave numbers. Here we could also use an enstrophy conserving scheme for the equations of motion. Even in the case of equations with divergence, such schemes are known for their ability to control the higher end of the spectrum (Arakawa 1968). However, enstrophy conservation is a constraint on the rotational part of the wind only. In the present case, the noise generated by the existence of internal boundaries can be described as a small-scale gravity wave with a strong divergent part; hence it cannot be controlled by formal enstrophy conservation. We may try instead to add a linear viscosity term to the equations of motion, such as $\nu\nabla^2\mathbf{V}$. An effective dissipation of the noise would then require an unrealistic value of the diffusion coefficient, which should be slightly greater than $10^6 m^2 \cdot s^{-1}$. In this case, viscous decay would predominate over nonlinear interactions over a large band of the spectrum.

Even though some physically meaningful two-grid interval waves may exist when our method is used in a primitive equation model including energy sources, we are not able to separate them from the artificial boundary effect. Furthermore, a nonstaggered centered scheme is unable to resolve the two-grid interval wave. Damping

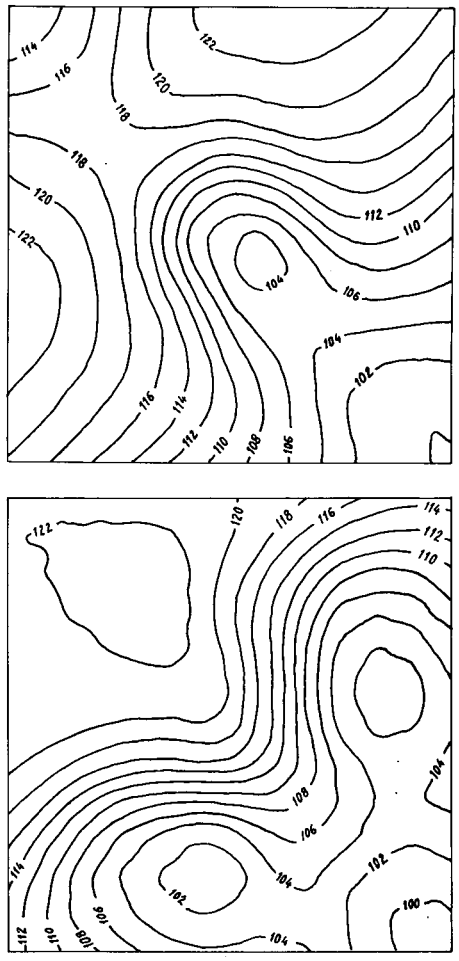

FIGURE 4.—Results from a numerical integration under the same conditions as in figure 3B with a selective damping by a term $\alpha\nabla^6 V$. Units are $10^3 \cdot m^2 \cdot s^{-2}$.

them out in any artificial manner would not cause a significant loss of information, provided the remaining part of the spectrum is not affected. A highly selective damping operator such as an iterated Laplacian would be adequate for this purpose. A term $\alpha\nabla^6\mathbf{V}$ added from time to time to the equations of motion would remove all the energy that may be generated at the two-grid interval wavelength. Inasmuch as its damping effect is proportional to the sixth power of the wave number, the corresponding dissipation elsewhere in the spectrum should be small compared to the effect of the nonlinear terms. Results from a last experiment, including a damping of this kind, are shown in figure 4. The main wave is not significantly affected by the removal of the noise.

7. CONCLUSION

The method we have described here is successful in removing all singularities from the finite-difference approximations of the equations of atmospheric motion on quasi-uniform spherical grids. The problem that remains yet is a truncation error problem resulting from the

presence of artificial internal boundaries in the calculation. We could have given conditions for enstrophy conservation in the case of a nondivergent flow, similar to the conditions given by Arakawa (1966, 1968) and Sadourny and Morel (1969). Such conditions would reduce to a special form of the curl* operator. However, this would require the use of a staggered grid, which may lead to larger truncation errors on the boundaries.

ACKNOWLEDGMENTS

We wish particularly to thank P. Morel, of the University of Paris, for his active support during the course of this study. We also thank the staff of the computing facility of the Centre National d'Etudes Spatiales, Brétigny, for making computing time available.

REFERENCES

Arakawa, A., "Computational Design for Long-Term Numerical Integration of the Equations of Fluid Motion: Two Dimensional Incompressible Flow, Part I," *Journal of Computational Physics*, Vol. 1, No. 1, Academic Press, New York, N.Y., Aug. **1966**, pp. 119–143.

Arakawa, Akio, "Numerical Simulation of Large Scale Atmospheric Motions, Numerical Solution of Field Problems in Continuum Physics," *Proceedings of a Symposium in Applied Mathematics, Durham, North Carolina, 1968*, American Mathematical Society, Providence, R.I., **1970**, pp. 24–40.

Kurihara, Yoshio, "Numerical Integration of the Primitive Equations on a Spherical Grid," *Monthly Weather Review*, Vol. 93, No. 7, July **1965**, pp. 399–415.

Kurihara, Yoshio, and Holloway, J. Leith, Jr., "Numerical Integration of a Nine-Level Global Primitive Equations Model Formulated by the Box Method," *Monthly Weather Review*, Vol. 95, No. 8, Aug. **1967**, pp. 509–530.

Phillips, Norman A., "Numerical Integration of the Primitive Equations on the Hemisphere," *Monthly Weather Review*, Vol. 87, No. 9, Sept. **1959**, pp. 333–345.

Sadourny, Robert, Arakawa, Akio, and Mintz, Yale, "Integration of the Nondivergent Barotropic Vorticity Equation With an Icosahedral-Hexagonal Grid for the Sphere," *Monthly Weather Review*, Vol. 96, No. 6, June **1968**, pp. 351–356.

Sadourny, Robert, and Morel, Pierre, "A Finite-Difference Approximation of the Primitive Equations for a Hexagonal Grid on a Plane," *Monthly Weather Review*, Vol. 97, No. 6, June **1969**, pp. 439–445.

Williamson, David, "Integration of the Barotropic Vorticity Equation on a Spherical Geodesic Grid," *Tellus*, Vol. 20, No. 4, Stockholm, Sweden, Nov. **1968**, pp. 642–653.

Williamson, David, "Integration of the Primitive Barotropic Model Over a Spherical Geodesic Grid," *Monthly Weather Review*, Vol. 98, No. 7, July **1970**, pp. 512–520.

[*Received March 16, 1971; revised September 7, 1971*]